Journal of Organometallic Chemistry, 328 (1987) 133–154
Elsevier Sequoia S.A., Lausanne – Printed in The Netherlands

ELECTROOXIDATION OF METAL CARBONYL ANIONS. FORMATION AND REACTIVITY OF 17-ELECTRON MANGANESE(0) RADICALS *

D.J. KUCHYNKA, C. AMATORE ** and J.K. KOCHI*

Department of Chemistry, University of Houston University Park, Houston, Texas 77004 (U.S.A.)

(Received January 3rd, 1987)

Summary

The series of carbonylmanganese anions $Mn(CO)_3P_2^-$, with P = phosphites and phosphines, undergo reversible anodic oxidation to the 17-electron radicals $Mn(CO)_3P_2^{\cdot}$ in tetrahydrofuran solutions. The reactivity of the carbonyl-manganese radicals of $Mn(CO)_3P_2^{\cdot}$ is evaluated in the context of hydrogen atom transfer from tributyltin hydride. The donor properties of the carbonylmanganates are strongly modulated by the ligands – the reversible oxidation potentials $E_{1/2}$ of phosphine-substituted anions being significantly more negative than those of the phosphite analogs. By contrast the reactivity of the phosphine- and phosphite-substituted radicals are not differentiated by electronic factors. However steric effects (as indicated by the cone angle of the phosphite or phosphine ligand) play a strong role in determining the reactivity of these 17-electron radicals. The combination of cyclic voltammetry, chronoamperometry, coulometry, and product analysis is used to establish the mechanism of hydrogen transfer from tributyltin hydride to $Mn(CO)_3P_2^{\cdot}$ in THF solutions. The measurement of the second-order rate constants k_2 for hydrogen transfer by double potential step chronoamperometry (DPSC) is described.

Introduction

The activation of metal carbonyls and derivatives is enhanced considerably upon the conversion to their paramagnetic species with an odd number of valence electrons [1,2]. Such transient intermediates are designated as carbonylmetal radicals, and they can be generated from stable diamagnetic metal carbonyls by electron transfer [3,4]. Among the various methods available for the generation of metalorganic radicals, we believe that electrochemical techniques offer the versatility of readily tunable potentials to adjust the driving force for electron transfer. Particu-

* Dedicated to Professor Jean Tirouflet on the occasion of his retirement.

** Present address: Laboratoire de Chimie, Ecole hormele Superieure, Paris, France 75231 Cedex 05.

0022-328X/87/$03.50

larly pertinent is the possibility of oxidizing carbonylmetallate anions [5,6], a wide variety of which is readily accessible [7–11]. Accordingly, we focus in this study on the electrochemical generation and reactivity of 17-electron carbonylmanganese radicals generated transiently upon the oxidation of the corresponding stable diamagnetic anions [12–16]. We chose the series of di-substituted derivatives $Mn(CO)_3P_2^-$, where P = trialkyl and triaryl phosphines and phosphites, since the 17-electron radicals are already known in this system [17].

Results

Synthesis of carbonylmanganate anions

The carbonylmanganate anions $Mn(CO)_3P_2^-$ were synthesized by either of three independent methods. Thus a THF solution of the bromomanganese(I) precursor $Mn(CO)_3P_2Br$ [18] was stirred with 1% sodium amalgam for 12 h, and the product isolated as the air-sensitive, sodium salt $Na^+Mn(CO)_3P_2^-$ according to the procedure of Hieber and coworkers [14]. More conveniently, we found that the carbonylmanganate anions were prepared in situ by the cathodic reduction of $Mn(CO)_3P_2Br$ at the potentials listed in Table 1. Coulometric measurement of the cathodic reduction at constant potential indicated the uptake of 2.00 ± 0.05 coulombs of charge per mole of $Mn(CO)_3P_2Br$ according to the stoichiometry in eq. 1.

$$Mn(CO)_3P_2Br + 2e \rightarrow Mn(CO)_3P_2^- + Br^- \quad (1)$$

The infrared spectra in Table 2 of the yellow carbonylmanganate anions generated quantitatively in this manner were identical with those obtained from the amalgam reduction (see Experimental). The carbonylmetallates could also be prepared by deprotonation of the readily available hydrides $HMn(CO)_3P_2$ with potassium t-butoxide in acetonitrile solution, viz.

$$HMn(CO)_3P_2 + K^+OBu\text{-}t^- \rightarrow K^+Mn(CO)_3P_2^- + HOBu\text{-}t \quad (2)$$

when P = tri-phenyl, *o*-tolyl, and isopropyl phosphite, and triphenylphosphine (see Experimental).

Anodic oxidation of carbonylmanganate anions to 17-electron radicals

The series of carbonylmanganate anions in Table 3 were oxidized electrochem-

TABLE 1

CYCLIC VOLTAMMETRIC POTENTIAL DATA FOR THE CARBONYLMANGANATE ANION $Mn(CO)_3P_2^-$ AND ITS DERIVATIVES [a]

Ligand P	$Mn(CO)_3P_2^-$ $E_{1/2}$	$Mn(CO)_3P_2^-$ E_p^a	$Mn(CO)_3P_2(THF)^+$ E_p^c	$Mn(CO)_3P_2Br$ E_p^c
Ph_3P	−0.94	−0.06	−1.87	−1.94
$(PhO)_3P$	−0.55	+0.37	−1.50	−1.91
$(o\text{-}CH_3C_6H_4O)_3P$	−0.59	+0.40	−1.60	−2.00
$(Ph_2PCH_2)_2$	−1.07	−0.10	−2.00	−2.11
$(n\text{-}Bu)_3P$	−1.20	−0.13	−1.80	−2.34
$(i\text{-}PrO)_3P$	−0.81	+0.14	−1.75	−2.26
$(i\text{-}Pr)_3P$	−1.22	−0.20	−2.15	−2.30

[a] In THF containing 0.3 *M* TBAP at $v = 500$ mV s^{-1}. V vs. SCE at 25°C. $E_{1/2}$ refers to half-wave potential, E_p^a irreversible anodic peak potential, and E_p^c irreversible cathodic peak potential. For a reversible CV wave, $E_{1/2} = E^0$.

TABLE 2

IR AND ^{1}H NMR SPECTRAL CHARACTERIZATION OF CARBONYLMANGANESE ANIONS AND DERIVATIVES [a]

Compound	ν(CO) (cm^{-1}) [a]	^{1}H NMR; δ (ppm) (J(P–H) (Hz)) [b]
$Mn(CO)_3[PPh_3]_2^-$ [d]	1769.9s, 1746.5s	
$Mn(CO)_3[PhO)_3P]_2^-$ [d]	1823.2s, 1805.9sh	
$Mn(CO)_3[DPPE]^-$ [d]	1867.2s; 1784.0sh; 1772.2s	
$Mn(CO)_3[o\text{-}CH_3C_6H_4O)_3P]_2^-$ [d]	1820.3s,s, 1801.6sh	
$Mn(CO)_3[(n\text{-}Bu)_2P]_2^-$ [d]	1739.5s, 1716.2s	
$Mn(CO)_3[(i\text{-}PrO)_3P]_2^-$ [d]	1779.1s, 1765.0sh	
$Mn(CO)_3[(i\text{-}Pr)_3P]_2^-$ [d]	1715.6s	
$HMn(CO)_3(PPh_3)_2$	1957.0w, 1916.5s,s	−7.30, t, (28.9)
$HMn(CO)_3[(PhO)_3P]_2$	2040.0vw, 1957.6s,s	−8.58, t, (50.0)
$HMn(CO)_3[DPPE]$	1994.8s,s, 1913.3s,s	−8.15, t, (46.4)
$HMn(CO)_3[(o\text{-}CH_3C_6H_4O)_3P]_2$	2039.4vw, 1954.2s,s	−8.50, t, (52.5)
$HMn(CO)_3[(n\text{-}Bu)_3P]_2$	1891.3s,s	−8.80, t, (31.7)
$HMn(CO)_3[(i\text{-}PrO)_3P]_2$	2014.4vw, 1929.1s,s; 1913.7sh	−8.35, t, (39.1)
$HMn(CO)_3[(i\text{-}Pr)_3P]_2$	1888.3s,s	−8.75, t, (32.0)
$Bu_3Sn\text{-}Mn(CO)_3[(PhO)_3P]_2$	2002.0w, 1959.8sh, 1934.0s	
$Bu_3Sn\text{-}Mn(CO)_3[(i\text{-}PrO)_3P]_2$ [c]	1971.5w, 1900.3s,s, 1887.5m	
$Bu_3Sn\text{-}Mn(CO)_3[(o\text{-}CH_3C_6H_4O)_3P]_2$	1998.4w, 1927.1s,s	
$Mn(CO)_3[PPh_3]_2Br$ [e]	2038.9w, 1952.2s,s, 1918.4m	
$Mn(CO)_3[(PhO)_3P]_2Br$ [e]	2068.2vw, 1994.0s,s, 1951.0m	
$Mn(CO)_3[DPPE]Br$ [e]	2025.5s,s, 1959.7s, 1917.4s	
$Mn(CO)_3[(o\text{-}CH_3C_6H_4O)_3P]_2Br$ [e]	2066.2w, 1991.0s,s, 1949.0m	
$Mn(CO)_3[(n\text{-}Bu)_3P]_2Br$ [e]	2025.4w, 1941.5s,s, 1896.5m	
$Mn(CO)_3[(i\text{-}PrO)_3P]_2Br$ [e]	2050.0w, 1964.0s,s, 1938.7m	
$Mn(CO)_3[(i\text{-}Pr)_3P]_2Br$ [e]	2019.3w, 1932.1s,s, 1887.1m	

[a] In THF solution unless indicated otherwise; s = strong; s,s = strong, sharp. [b] In $CDCl_3$. [c] In CH_2Cl_2. [d] As tetra-n-butylammonium salt. [e] In $CHCl_3$.

ically in 5×10^{-3} M THF solution containing 0.3 M tetra-n-butylammonium perchlorate (TBAP). At a constant potential of −0.5 V vs. SCE, the amount of charge passed was $Q = 1.0 \pm 0.1$ coulombs per mole of carbonylmanganate. Analysis of the anolyte by quantitative IR spectroscopy indicated the oxidative conversion

TABLE 3

ELECTROCHEMICAL PARAMETERS FOR THE CARBONYLMANGANATE REDOX COUPLE $Mn(CO)_3P_2^-/Mn(CO)_3P_2^{\cdot}$ IN THF SOLUTION [a]

Ligand P	$E_{1/2}$ (V vs. SCE)	α [b]	$k_oD^{-1/2}$ ($s^{-1/2}$) [c]	k_o ($cm\ s^{-1}$) [d]
$(i\text{-}PrO)_3P$	−0.81	0.80	0.49	1.1×10^{-3}
$(o\text{-}CH_3C_6H_4O)_3P$	−0.59	0.56	0.37	8.3×10^{-4}
$(PhO)_3P$	−0.55	0.56	0.75	1.7×10^{-3}
$(n\text{-}Bu)_3P$	−1.20	0.63	0.43	9.6×10^{-4}

[a] Containing 0.3 M TBAP and $[Mn(CO)_3P_2^-] = 5\times10^{-3}$ M at 25 °C. [b] From the slope of the plot of ΔE_p vs. log v. [c] From ref. 24. [d] With $\bar{D} = 5\times10^{-6}$ $cm^2\ s^{-1}$ (see ref. 23).

of the carbonylmanganate anion to the manganese hydride according to the partial stoichiometry in eq. 3.

$$Mn(CO)_3P_2^- - e \xrightarrow{[-0.5\ V]} HMn(CO)_3P_2, \text{ etc.} \quad (3)$$

Each of the manganese hydrides was characterized in the ^1H NMR spectrum by a high field triplet resonance at $\delta \sim -8$ (see Table 2).

In order to determine the origin of the hydridic ligand in eq. 3, we examined the transient electrochemical behavior of carbonylmanganate anions by cyclic voltammetry and double-step chronoamperometry. The initial positive scan cyclic voltammograms of some representative carbonylmanganate anions in Fig. 1 show that they all share two features in common.

(a) The more negative anodic peak (labelled P_1) corresponds to the 1-electron oxidation of $Mn(CO)_3P_2^-$ to the 17-electron carbonylmanganese radical by the

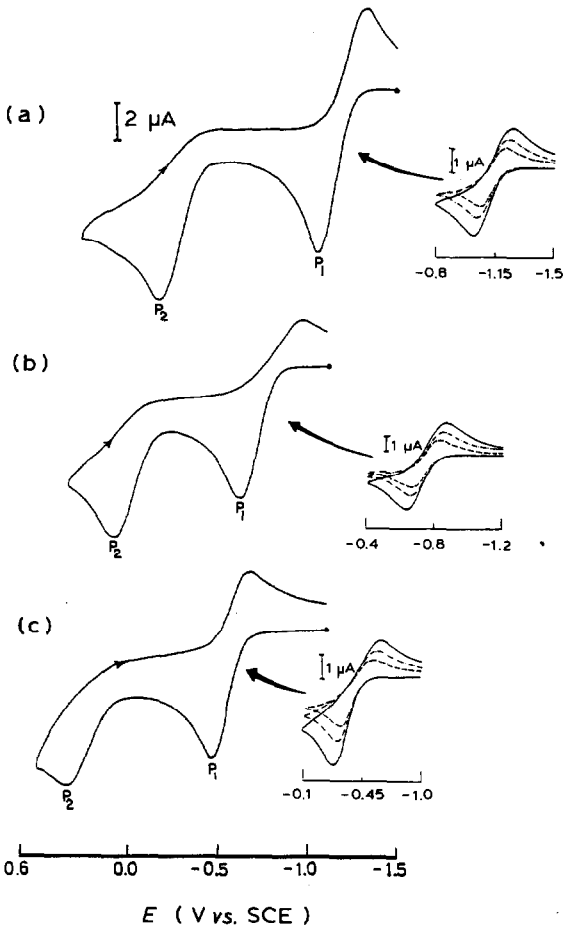

Fig. 1. Initial positive scan cyclic voltammogram of 5×10^{-3} *M* carbonylmanganate in THF containing 0.4 *M* TBAP at 500 mV s^{-1}. (a) $Mn(CO)_3(Bu_3P)_2^-$, (b) $Mn(CO)_3[(i\text{-}PrO)_3P]_2^-$ and $Mn(CO)_3[(PhO)_3P]_2^-$. The insets show the $Mn(CO)_3P_2^-/Mn(CO)_3P_2$ couple at $v = 200$ (———), 100 (·–·–·) and 50 (- - - - -) mV s^{-1}.

calibration of the peak current with ferrocene, i.e.

$$Mn(CO)_3P_2^- \rightleftharpoons Mn(CO)_3P_2^{\cdot} + e \quad (4)$$

The chemically reversible process is indicated by the anodic and cathodic peak current ratios $i_a/i_c = 1.0$ at sweep rates $v \geq 20$ mV s^{-1} in cyclic voltammetry, and $i_a/i_c = 0.293$ at step times $\theta \leq 1$ s in double potential step chronoamperometry [19–23]. The separation ΔE_p of the anodic and cathodic peak potentials $E_p^a - E_p^c \geq$ 100 mV indicated a somewhat slow charge transfer in eq. 4. Indeed the plots of the peak separation ΔE_p vs. log v shown in Fig. 2 are linear, characteristic of the CV wave P_1 which is partially controlled by the kinetics of electron transfer as well as by diffusion [24]. The electrochemical parameters of the carbonylmanganese radicals obtained from plots such as those shown in Fig. 2 are listed in Table 3. The EPR spectra of the carbonylmanganese radicals [25] from eq. 4 can be readily observed after electrooxidation of $Mn(CO)_3P_2^-$ with P = tri-n-butylphosphine and tri-isopropyl phosphite.

(b) Upon the continued positive potential scan in Fig. 1, a second anodic wave labelled P_2 is observed which is also common to all the carbonylmanganese anions. The 1-electron peak P_2 is irreversible, and it corresponds to the further oxidation of the 17-electron radical $Mn(CO)_3P_2^{\cdot}$ as described earlier [26]. The CV irreversibility arises from the enhanced reactivity of the coordinatively unsaturated 16-electron cation $Mn(CO)_3P_2^+$, which rapidly incorporates a solvent molecule, i.e.

$$Mn(CO)_3P_2^{\cdot} \rightarrow Mn(CO)_3P_2^+ + e \quad (5a)$$

$$Mn(CO)_3P_2^+ + THF \xrightarrow{fast} Mn(CO)_3P_2(THF)^+ \quad (5b)$$

The latter can be observed upon the return sweep as a new cathodic wave, the irreversible peak potential E_p of which is listed in Table 1.

The electrosynthesis of the manganese hydride in eq. 3 and the formation of the

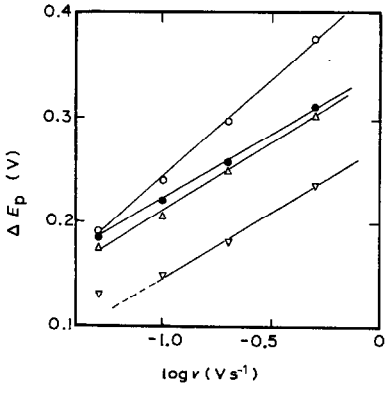

Fig. 2. Variation of ΔE_p with log$v$ for the reversible anodic oxidation of $Mn(CO)_3[(i\text{-}PrO)_3P]_2^-$ ○, $Mn(CO)_3[(o\text{-}CH_3C_6H_4O)_3P]_2^-$ ●, $Mn(CO)_3(Bu_3P)_2^-$ △ and $Mn(CO)_3[(PhO)_3P]_2^-$ ▽ in THF containing 0.4 *M* TBAP at 25 °C.

carbonylmanganese radical at the same potential (eq. 4) are directly interrelated by a process involving hydrogen atom abstraction, i.e.

$$Mn(CO)_3P_2^{\cdot} + HS \rightarrow HMn(CO)_3P_2 + S^{\cdot} \quad (6)$$

where HS is the THF solvent and/or supporting electrolyte. Indeed such a homolytic process does account for the observation of butene-1 and tributylamine when tetra-n-butylammonium salts are used as the supporting electrolyte [27,28]. Furthermore this mechanism for hydride formation can be reconciled with the observed potentiostatic coulometry of 1.0 faraday during the bulk electrolysis in eq. 3 if the radical S· disappears in a bimolecular step such as coupling or disproportionation [26,29]. However, owing to the ambiguity as to the hydrogen source in eq. 6, we reexamined the electrochemistry in the presence of tri-n-butylstannane which is known to be a powerful hydrogen atom donor [29], i.e.

$$Mn(CO)_3P_2^{\cdot} + HSnBu_3 \rightarrow HMn(CO)_3P_2 + Bu_3Sn^{\cdot} \quad (7)$$

Electrooxidation of carbonylmanganese anions in the presence of hydrogen donor

The electrooxidations of carbonylmanganate anions in THF solutions containing tri-n-butyltin hydride proceed smoothly at −0.5 V similar to those in eq. 3. The presence of manganese hydride in the anolyte was indicated by their characteristic carbonyl bands (Table 2). Furthermore when tri-n-butyl deuteride was used as the hydrogen source, the high field triplet resonances in the ^1H NMR spectra were replaced with analogous partially resolved triplets in the ^2H NMR spectrum (see Experimental). Isotopic labelling thus indicates that the stannane is the sole source of the hydride ligand, i.e.

$$Mn(CO)_3P_2^- - e \xrightarrow[Bu_3SnD]{[-0.5\ V]} DMn(CO)_3P_2, \text{ etc.} \quad (8)$$

In addition, the tri-n-butylstannyl moiety is detected either as hexa-n-butyldistannane or the manganese derivative $Bu_3SnMn(CO)_3P_2$ (Table 4). The presence of hexa-n-butyldistannane is established by GC-MS analysis, but the amounts formed are only noted qualitatively in Table 4 owing to analytical problems arising from

TABLE 4

PRODUCT DISTRIBUTIONS FROM THE ELECTROOXIDATION OF CARBONYLMANGANATE ANIONS $Mn(CO)_3P_2^-$ IN THE PRESENCE OF Bu_3SnH [a]

Ligand P	n_{app} [b]	$HMn(CO)_3P_2$ (%) [c]	$Bu_3SnMn(CO)_3P_2$ (%) [c]	$Bu_3SnSnBu_3$ [d]
Ph_3P	0.3	100	0	++
$(PhO)_3P$	1.0	55	45	tr
$(o\text{-}CH_3C_6H_4O)_3P$	1.0	70	30	+
DPPE	0.4	100	0	++
$(OBu)_3P$	0.3	100	0	++
$(i\text{-}PrO)_3P$	1.0	50	50	0

[a] In THF solution containing 0.3 *M* TBAP, 5×10^{-3} *M* Bu_3SnH, and 5×10^{-3} *M* carbonylmanganate as tetra-n-butylammonium salt at 22°C. Potentiostatic electrolysis at the potential for $Mn(CO)_3P_2^-$ in Table 1. [b] From coulometry relative to carbonylmanganate charged. [c] By IR analysis, see Table 2. [d] Approximated yields (see text): ++ = major (stoichiometric) amount, + = minor amounts, tr = traces.

severe chromatographic tailing. The yields of $Bu_3SnMn(CO)_3P_2$ listed in Table 4 were determined by quantitative IR analysis using the characteristic carbonyl bands of authentic samples (Table 2) prepared independently from the carbonylmanganate anion [15], i.e.

$$Mn(CO)_3P_2^- + Bu_3SnCl \rightarrow Bu_3Sn\text{–}Mn(CO)_3P_2 + Cl^- \quad (9)$$

The complete isotopic incorporation of deuterium into the manganese hydride in eq. 8 derives from the 17-electron radicals as intermediates which are effectively trapped by tri-butyltin hydride immediately following electrooxidation of the anion, i.e.

Scheme 1

$$Mn(CO)_3P_2^- - e \overset{k_s}{\rightleftarrows} Mn(CO)_3P_2\cdot \quad (10)$$

$$Mn(CO)_3P_2\cdot + Bu_3SnH \overset{k_2}{\longrightarrow} HMn(CO)_3P_2 + Bu_3Sn. \quad (11)$$

The formation of the other products, viz., hexa-butyldistannane and the stannyl-manganese carbonyl, are also consistent with the subsequent homo- and cross-dimerization of the stannyl radicals [30].

$$Bu_3Sn\cdot \xrightarrow{Bu_3Sn\cdot} Bu_3Sn\text{–}SnBu_3 \quad (12)$$

$$Bu_3Sn\cdot \xrightarrow{Mn(CO)_3P_2\cdot} Bu_3Sn\text{–}Mn(CO)_3P_2 \quad (13)$$

The sequence of steps in Scheme 1 readily account for the marked effect the presence of Bu_3SnH has on the reversible cyclic voltammogram of the carbonyl-manganate anion. Figure 3 shows the monotonic diminution in the peak current ratio i_c/i_a with successive increments of Bu_3SnH. [Note the anodic and cathodic

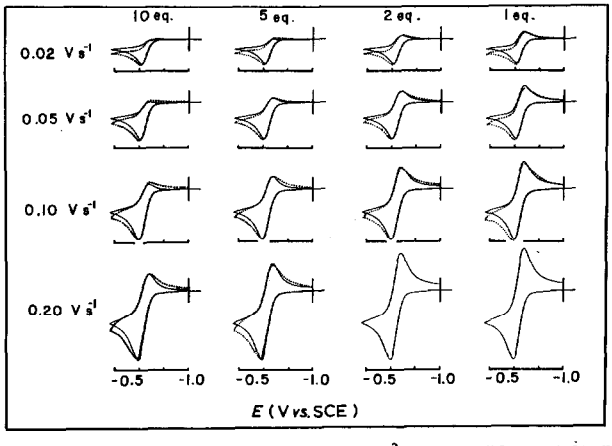

Fig. 3. Cyclic voltammograms of 5×10^{-3} *M* $Mn(CO)_3[(PhO)_3P]_2^-$ in THF containing 0.3 *M* TBAP and Bu_3SnH (as indicated) at various sweep rates. The computer simulated cyclic voltammograms (· · · · · ·) based on $k_2 = 7.3\ M^{-1}\ s^{-1}$ (see text).

currents are directly related to the concentrations of the anion $Mn(CO)_3P_2^-$ and the radical $Mn(CO)_3P_2^{\cdot}$, respectively, in the region about the electrode.] The matrix of cyclic voltammograms reveals that the concentration of the radicals in the diffusion layer decreases with incremental additions of tributylstannane, and that an equivalent variation is achieved simply by changing the CV sweep rate v. In other words the lifetime of the initially formed radical is exceedingly short in the presence of Bu_3SnH, as seen by the return cathodic wave which is either severly diminished or absent [31]. The bimolecular nature of the interception of $Mn(CO)_3P_2^{\cdot}$ by tributylstannane (eq. 11) is established by the fit of the theoretical cyclic voltammograms (dotted curves) which represent digital simulations [20] of the kinetics according to the mechanism in Scheme 1 (see Experimental).

Rate constants for hydrogen atom transfer from stannane to carbonylmanganese radicals

The reactivity of carbonylmanganese radicals is reflected in the hydrogen atom transfer from tributylstannane in Scheme 1. In order to obtain a quantitative measure of this homolytic reactivity, we used transient electrochemical methods to evaluate the second-order rate constant k_2 in eq. 11. Kinetic analysis by cyclic voltammetry as in Fig. 2 is of limited value since the heterogeneous rates of electron transfer for the $Mn(CO)_3P_2^-/Mn(CO)_3P_2^{\cdot}$ couple are relatively slow (vide supra). [The latter complicates the overall kinetics and results in a poor CV sensitivity for assessing the homogeneous rates.] Accordingly, we examined double potential step chronoamperometry (DPSC) as the kinetics method of choice for this system since it is not dependent on the magnitude of k_0 (eq. 10) [19–22, 32].

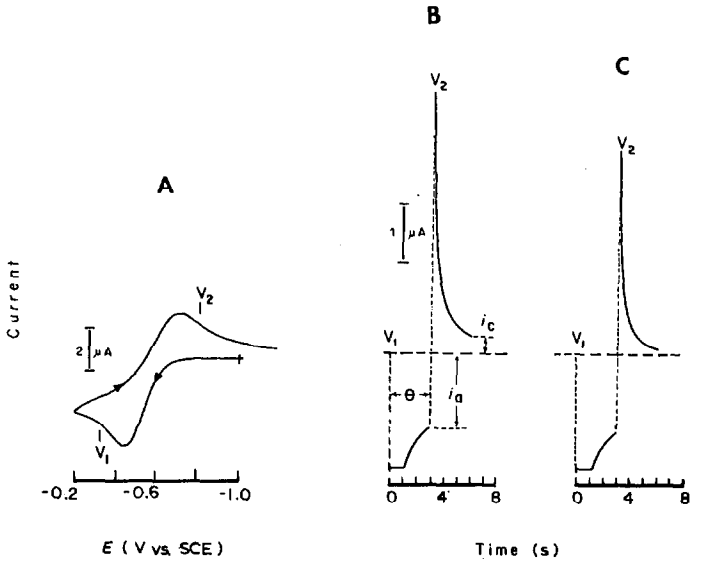

Fig. 4. Double potential step chronoamperometry (DPSC) of 5×10^{-3} *M* $Mn(CO)_3[(o\text{-}CH_3C_6H_4O)_3P]_2^-$ in THF containing 0.3 *M* TBAP. (A) Cyclic voltammogram at 300 mV s^{-1} showing the locations of V_1 V_2 with no added Bu_3SnH. (B) DPSC with $\theta = 3$ s (no added Bu_3SnH). (c) DPSC with $\theta = 3$ s and 20 equiv. added Bu_3SnH.

An aliquot of a freshly prepared solution of $Mn(CO)_3P_2^-Bu_4N^+$ was added to a CV cell sufficient to make up a 5×10^{-3} M solution in THF. The DPSC experiments were performed on solutions containing incremental amounts of tributylstannane from 1 to 20 equivalents. In a representative run the first pulse was applied at a potential 100 mV positive of E_p^a and held for a time interval θ. A second pulse was then stepped at a potential 100 mV negative of E_p^c and held for θ s. The ratio i_c/i_a was calculated from cathodic and anodic currents designated as i_c and i_a respectively, in Fig. 4. The typical decrease in the cathodic current attendant upon the addition of tributylstannane is illustrated by a comparison of Fig. 4b and 4c. When $[Bu_3SnH]$ was varied, the ratio i_c/i_a could be maintained constant by choosing θ such that $\theta[Bu_3SNH]$ was constant. From this behavior we deduced that the kinetics order for tributylstannane was one. On the other hand, when $[Mn(CO)_2P_2^-]$ was varied, no variation of i_c/i_a was observed, which showed that the kinetics order in the carbonylmanganese anion was zero. Thus the kinetics expression for the chemical process is

$$-d[Mn(CO)_3P_2^{\cdot}]/dt = k^{app}[Mn(CO)_3P_2^{\cdot}][Bu_3SnH] \quad (14)$$

where the second-order rate constant k^{app} is independent of $[Bu_3SnH]$ and $[Mn(CO)_3P_2^-]$. The smooth curves obtained from the (normalized) current ratios R measured at various step times as a function of $\log[Bu_3Sn]\theta$ are shown in Figs. 5A–5E. These experimental curves were compared with the theoretical working curves (see Experimental), in which the ordinate also contains the second-order rate constant k_2 as shown in Fig. 5F.

It is important to note that as a requirement for the mechanistic scheme considered, the product $i_a(\theta)^{1/2}$ must be independent of the step time since the electron consumption n_{app} is independent of the presence of BuSnH (vide supra). Indeed Fig. 6 illustrates the linear plots of i_a against $(\theta)^{-1/2}$ with zero intercepts

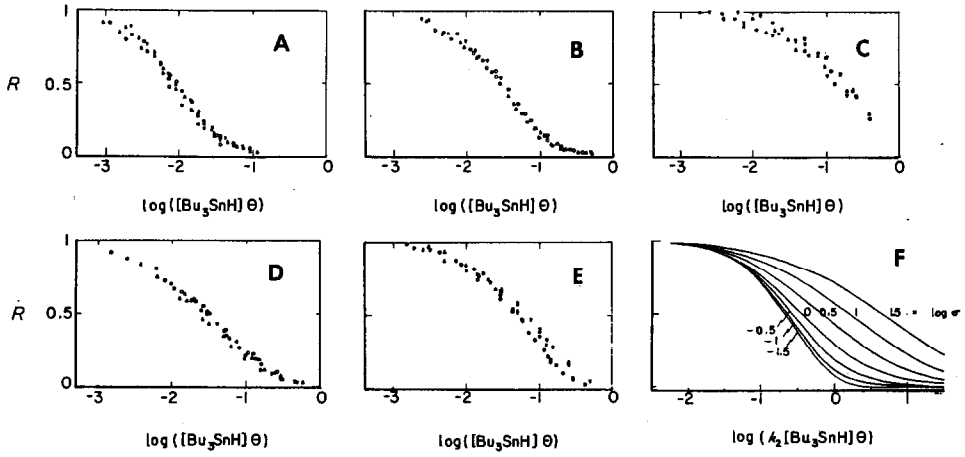

Fig. 5. Experimental variation of the normalized anodic current (R) with Bu_3SnH concentration and step times θ for (A) $Mn(CO)_3(DPPE)^-$, (B) $Mn(CO)_3[(PhO)_3P]_2^-$, (C) $Mn(CO)_3[(o\text{-}CH_3C_6H_4O)_3P]_2^-$, (D) $Mn(CO)_3(Bu_3P)_2^-$ and (E) $Mn(CO)_3[(i\text{-}PrO)_3P]_2^-$ in THF containing 0.3 M TBAP at 22°C. (F) The theoretical current variation with $\log k_2[Bu_3SnH]\theta$ at various values of the kinetic parameter σ, as described in the text.

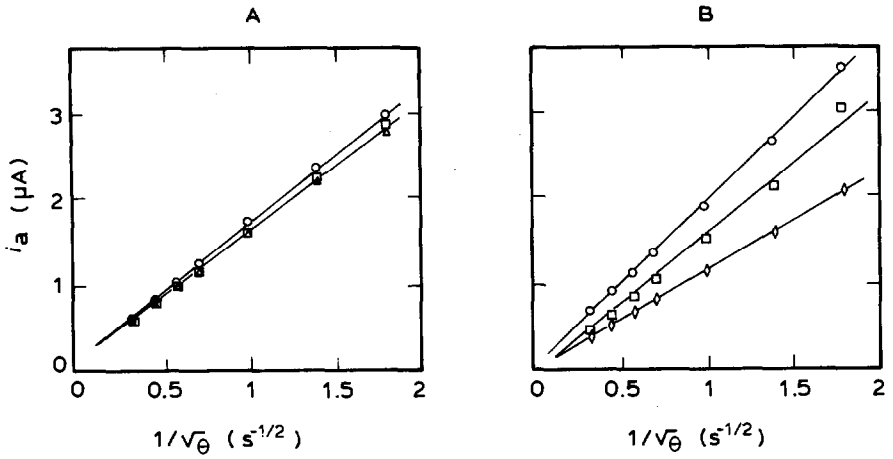

Fig. 6. Single step chronoamperometry of 5×10^{-3} *M* THF solutions of (A) $Mn(CO)_3[(o\text{-}CH_3C_6H_4O)_3P]_2^-$ and (B) $Mn(CO)_3(Bu_3P)_2^-$ in the presence of ○ no, □ 2 equiv., ◇ 5 equiv, or △ 10 equiv of added Bu_3SnH. See text.

[23]. [Note that the slopes of the phosphine-substituted anions decreased with time.] The observation of the linear behavior with zero intercepts indicates that an electrocatalytic process is unimportant in the timescale of the double step experiment. This contrasts with the results of bulk electrolysis (Table 4) in which the longer timescale allows the incursion of a themal side reaction (eq. 20, vide infra).

The temperature dependence of the second-order rate constant k_2 was measured between 0 and 45 °C. Plots of $\ln k_2$ and temperature (T^{-1}) gave values for the enthalpies and entropies of activation as $\Delta H^{\ddagger} = 11.2 \pm 0.3$ kcal mol^{-1} and $\Delta S^{\ddagger} = -19 \pm 1$ cal mol^{-1} deg^{-1} for $Mn(CO)_3[(o\text{-}CH_3C_6H_4O)_3P]_2^{\cdot}$ and $\Delta H^{\ddagger} = 10.0 \pm 0.4$ kcal mol^{-1} and $\Delta S^{\ddagger} = -12.5 \pm 0.9$ cal mol^{-1} deg^{-1} for $Mn(CO)_3[(n\text{-}Bu)_3P]_2^{\cdot}$.

Discussion

Electrooxidation of the carbonylmanganese anions $Mn(CO)_3P_2^-$ occurs in THF solution with the uptake of 1.0 faraday of charge to produce the metastable 17-electron radical $Mn(CO)_3P_2^{\cdot}$ according to eq. 4. ESR analysis of the anolyte affords slightly broadened spectra but with *g*-values akin to those of the same or related carbonylmanganese radicals reported by Brown and others [25,33].

All of these solutions upon standing until the radical disappears (by monitoring either the IR or ESR spectra) result in the formation of the corresponding manganese hydride $HMn(CO)_3P_2$ [34] in essentially quantitative yields (eq. 3). The reactivity of the various carbonylmanganese radicals generated in this way roughly parallels the trend in the second-order rate constants listed in Table 5, i.e., $i\text{-}Pr_3P > Ph_3P > (o\text{-}CH_3C_6H_4O)_3P > (i\text{-}PrO)_3P > (PhO)_3P > n\text{-}Bu_3P >$ DPPE. In these experiments, the hydridic ligand present in $HMn(CO)_3P_2$ may derive from either the solvent (THF), the supporting electrolyte (TBAP), or both. However this ambiguity is readily removed by the deliberate addition of a powerful hydrogen atom donor; and the manganese hydride obtained from tributyltin deuteride in eq. 8 is exclusively the isotopically labelled $DMn(CO)_3P_2$. The other products generated in the preparative

TABLE 5

SECOND-ORDER RATE CONSTANT k_2 FOR HYDROGEN TRANSFER TO $Mn(CO)_3P_2^{\cdot}$ FROM Bu_3SnH [a]

Ligand P	k_2 ($M^{-1}\,s^{-1}$) [b]	log σ [c]	θ [d] (cm^{-1})	Cone angle (deg) [e]
$(PhO)_3P$	8.1	−1.0	2085.3	128
$(o\text{-}CH_3C_6H_4O)_3P$	2.1	0.0	2084.1	141
DPPE	25.1 (28.3)	−1.0	2066.7 [f]	125 [g]
$(n\text{-}Bu)_3P$	13.2	0.0	2060.3	132
$(i\text{-}PrO)_3P$	5.0 (4.6)	−0.5	2075.9	130
Ph_3P	~ 0.5	>1	2068.9	145
$i\text{-}Pr_3P$	< 0.01	>1.5	2059.7	160

[a] By DPSC method in THF solution containing 0.3 *M* TBAP at 25 °C. [b] Estimated accuracy ±15%. Numbers in parentheses refer to Bu_3SnD. [c] $\sigma = k_{-2}/2k_3$ (see text). [d] Carbonyl stretching band (A_1 mode) in $Ni(CO)_3P$ in ref. 36. [e] Cone angle from ref. 36. [f] For Ph_2EtP. [g] Assuming angle (P–Mn–P) = 85°.

scale electrolysis of $Mn(CO)_3P_2^-$ in the presence of Bu_3SnH are dependent on the nature of the ligand P, as shown in Table 4. Accordingly the distinctive behavior of the phosphite- and phosphine-substituted radicals is discussed individually below.

Reactivity of phosphite-substituted carbonylmanganese(0) radicals

The electrooxidation of the phosphite-substituted carbonylmanganese anions show clean oxidative behavior with $n_{app} = 1.0$, and the stoichiometry is approximated as

$$2Mn(CO)_3P_2^- - 2e \xrightarrow[Bu_3SnH]{} HMn(CO)_3P_2 + Bu_3SnMn(CO)_3P_2 \qquad (15)$$

Minor amounts of hexabutylditin are detected when the yield of the hydridomanganese carbonyl exceeds that of the stannyl derivative (see Table 4). These products and the observed coulometry are consistent with the mechanistic formulation in Scheme 1. Accordingly the kinetic working curves for the double potential step chronoamperometry are derived with the rate constants in Scheme 2 [35].

Scheme 2

$$Mn(CO)_3P_2^- \rightleftharpoons Mn(CO)_3P_2^{\cdot} + e \qquad (16)$$

$$Mn(CO)_3P_2^{\cdot} + Bu_3SnH \underset{k_{-2}}{\overset{k_2}{\rightleftharpoons}} HMn(CO)_3P_2 + Bu_3Sn^{\cdot} \qquad (17)$$

$$Bu_3Sn^{\cdot} + Mn(CO)_3P_2^{\cdot} \xrightarrow{k_3} Bu_3SnMn(CO)_3P_2 \qquad (18)$$

Hydrogen transfer in eq. 17 provides the basis for assessing the reactivity of the 17-electron carbonylmanganese radicals. Indeed the second-order rate constant k_2 for hydrogen transfer to the 17-electron radical is contained explicity in the kinetic analysis of the DPSC experiments. Thus in Fig. 5, k_2 is included in the ordinate as the function $k_2[Bu_3SnH]\theta$, and the abscissa is the normalized current ratio $R = (i_a/i_c)/0.293$. The associated kinetic parameter in Fig. 5F is $\sigma = k_{-2}/2k_3$. Qualitatively, the steepness of the theoretical working curves in Fig. 5F is governed by the

intrinsic value of second-order rate constant k_2 for hydrogen abstraction (eq. 17), while the overall shape of the curve is governed by the value of logσ. In all cases, we obtain excellent overlaps of the experimental plots and the theoretical curve with only minor deviation, and this underscores the essential validity of Scheme 2. In a limiting kinetic situation at which $\sigma_{lim} \rightarrow \infty$, hydrogen transfer acts as a preequilibrium and k_2 cannot be evaluated directly. Under these conditions the dependence of R on [BuSnH]θ involves the kinetic parameter $\sigma' = k_3 k_2 / k_{-2}$. In practice, two of the carbonylmanganese radicals display rather large values of logσ, namely $Mn(CO)_3(PPh_3)_2$ and $Mn(CO)_3[i\text{-}Pr_3P]_2$ which afford $\sigma' = 5.8 \times 10^{-2}$ and $6.3 \times 10^{-2}\ M^{-1}\ s^{-1}$, respectively. This distinction presumably derives from steric factors since these derivatives also contain ligands with the largest cone angles ($PPh_3 = 145°$, $i\text{-}Pr_3P = 160°$) [36]. Let us also consider other mechanistic variations of Scheme 2. When the kinetic parameter $\sigma_{lim} \rightarrow 0$, hydrogen transfer is irreversible. This leads to a very steep dropoff in the theoretical working curve which is clearly at variance with the experimental plots in Fig. 5A–5E. When the cross-coupling process in eq. 18 is replaced with a homo coupling of stannyl radicals (eq. 12), kinetic analysis leads to a dependence of R on the square of tributylstannane concentration – which is again at variance with the experimental data. Moreover when both the homo and cross coupling are included in the kinetic analysis, very poor fits to the experimental curves result. Similarly if hydrogen transfer is treated as a preequilibrium and the radical couplings (eqs. 12 and 18) is made rate-limiting, the dependence on $[Bu_3SnH]^2$ is predicted. The possibility of $Bu_3Sn^{\cdot}$ being involved via a pathway other than homolytic coupling can be considered but it is readily discarded, since it is inconsistent with the results of bulk electrolysis. Finally the second-order rate constant k_2 for $Mn(CO)_3(Bu_3P)_2^{\cdot}$ in Table 5 is in excellent agreement with that obtained by Brown and McCullen using an IR technique [17]. However our rate constant for $Mn(CO)_3[i\text{-}PrO)_3P]_2$ is ~ 30 times larger than that evaluated previously. Part of the discrepancy may be related to our observation of large amounts of the stannyl complex $Bu_3SnMn(CO)_3[(i\text{-}PrO)_3P]_2$ whereas its formation is not specified under the conditions reported by Brown and McCullen [17]. Unfortunately further comparisons are not possible, especially since the i-propyl derivative was the only phosphite examined in the earlier study.

The magnitudes of the second-order rate constant k_2 listed in Table 5 show variations with the steric size and the donor ability of the phosphorus(III) ligands as measured by the cone angles and the carbonyl stretching band (ν(CO)) in $Ni(CO)_3P$, respectively [36]. By these measures the difference between phenyl and *o*-tolyl phosphites is largely steric (see Table 5). Accordingly we attribute the 4-fold difference in rates of hydrogen transfer to steric encumberance about the paramagnetic manganese center by the pair of bulky tri-*o*-tolyl phosphite ligands.

Reactivity of phosphine-substituted carbonylmanganese radicals

The electrooxidation of the phosphine-substituted carbonylmanganese anions also shows clean oxidative behavior but with $n_{app} \cong 0.3$ and a stoichiometry approximated as

$$Mn(CO)_3P_2^- - e \xrightarrow[Bu_3SnH]{} HMn(CO)_3P + Bu_3SnSnBu_3 \qquad (19)$$

Unlike the phosphite-substituted analogs in eq. 15, the stannylmanganese carbonyl $Bu_3SnMn(CO)_3(phosphine)_2$ is not observed as a major product. Indeed the

absence of this stannylmanganese carbonyl can be related to its thermal instability. For example, when $Mn(CO)_3(Bu_3P)_2^-$ is treated with Bu_3SnCl in THF, the formation of a fleeting species is indicated by the observation of a transient carbonyl band at ν(CO) 1877 cm^{-1} in the IR spectrum. This species, tentatively identified as $Bu_3SnMn(CO)_3(Bu_3P)_2$ by analogy with the phosphite analogues formed in eq. 9, decays completely to the manganese hydride $HMn(CO)_3(Bu_3P)_2$ showing a single characteristic carbonyl band at ν(CO) 1891 cm^{-1} (Table 2) [34]. A similar observation was noted earlier by Onaka and coworkers [15a]. In addition, we find that significant amounts of hexabutylditin are formed together with an unidentified tin-containing product (see Experimental). From these qualitative observations we deduce that the phosphine-substituted stannylmanganese carbonyls spontaneously decompose according to the suggested stoichiometry.

$$Bu_3SnMn(CO)_3(phosphine)_2 \xrightarrow[Bu_3SnH]{} HMn(CO)_3(phosphine)_2 + Bu_3SnSnBu_3 \quad (20)$$

It is noteworthy that the difference in stability of $Bu_3SnMn(CO)_3(phosphine)_2$ relative to the phosphite analogues in eq. 9 parallels the effect these donor ligands have on the ease of Mn–Mn homolysis in $Mn_2(CO)_8P_2$. For example, Jackson and Poe [37] have convincingly shown that phosphine substitution into $Mn_2(CO)_{10}$ lowers the Mn–Mn bond strength by ~ 20 kJ mol^{-1} in $Mn_2(CO)_8(Bu_3P)_2$. By contrast, the metal–metal bond strengths in the analogous bis-phosphite substituted dimers $Mn_2(CO)_8[(MeO)_3P]_2$ and $Mn_2(CO)_8[(PhO)_3P]_2$ were nearly unaffected. Thus it can be argued that first-formed $Bu_3SnMn(CO)_3(phosphine)_2$ is thermodynamically unstable and readily decomposes homolytically to the more stable hydride derivative $HMn(CO)_3(phosphine)_2$. If so, the observed stoichiometry in eq. 19 actually represents a composite of two processes, namely, the stoichiometry observed with phosphite-substituted radicals in eq. 15 plus the stoichiometry for the decay of the stannylmanganese transient in eq. 20. Strong support for this conclusion derives from double potential step chronoamperometry of $Mn(CO)_3(phosphine)_2^-$ in the presence of Bu_3SnH. Thus the experimental working curves shown in Figs. 5A and 5D fit the same pattern as those obtained from the phosphite-substituted analogs. Most importantly the second-order rate constant $k = 13\ M^{-1}\ s^{-1}$ for $Mn(CO)_3(Bu_3P)_2$ obtained from Fig. 5 is in excellent agreement with the value of $k_2 = 11\ M^{-1}\ s^{-1}$ obtained by Brown and McCullen [17].

The trend in the reactivity of the phosphine-substituted radicals are also strongly influenced by the steric effects of the ligands, the magnitudes of k_2 decreasing in the order P = n-Bu_3P > Ph_3P > i-Pr_3P in line with their cone angles (see Table 5). From the analysis of the IR and ESR spectra of $Mn(CO)_3P_2$, Brown earlier concluded that phosphorus ligands occupy *trans*-basal positions in the square pyramidal structure with C_{2v} symmetry [25].

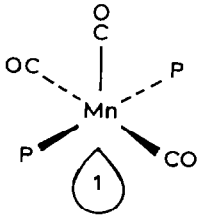

1

From such a structure of the radical it is conceivable that the presence of bulky phosphines would limit access to the manganese center by the tributyltin hydride. The absence of a deuterium kinetic isotope effect, determined within the accuracy of the DPSC method (see Table 5), suggests that the transition state for hydrogen transfer occurs far along the reaction coordinate. Such a transition state is also consistent with the enhanced reactivity of the chelated radical $Mn(CO)_3(DPPE)\cdot$ for which the second-order rate constant k_2 is > 50 times larger than that for P = triphenylphosphine (Table 5). The bidentate nature of DPPE forces the radical to adopt one of two configurations, i.e.

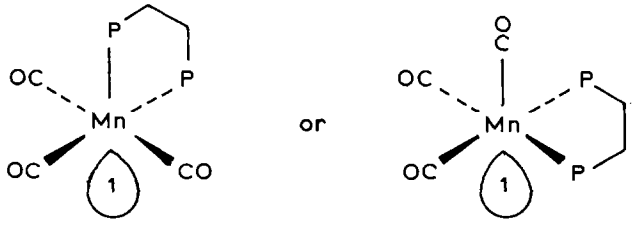

both of which are less sterically congested than the *trans*-basal structure above. Electronic effects of the phosphorus ligands on the reactivity of the 17-electron radicals appear to be rather minor. For example, tri-n-butylphosphine and triisopropyl phosphite have similar cone angles but differ in reactivity by less than a factor of three.

Hydrogen transfer to carbonylmanganate anions

The coulometry in Table 4 indicates that phosphine-substituted anions consistently consume much less than a stoichiometric number of electrons with $n_{app} \cong 0.3$. Since the oxidation of $Mn(CO)_3(phosphine)_2^-$ clearly represents an one-electron wave (compare Fig. 3), the low value of n_{app} strongly suggests the occurrence of a simultaneous thermal process in which $Mn(CO)_3(phosphine)_2^-$ is converted by Bu_3SnH to the manganese hydride $HMn(CO)_3(phosphine)_2$. Indeed when an equimolar mixture of $Mn(CO)_3(Bu_3P)_2^-$ and Bu_3SnH was allowed to stand for 24 h, the manganese hydride was formed in quantitative yield together with large but undetermined amounts (vide supra) of distannane, i.e.

$$Mn(CO)_3(phosphine)_2^- + Bu_3SnH \xrightarrow{k_t} HMn(CO)_3(phosphine)_2 + Bu_3SnSnBu_3, \text{ etc.} \quad (21)$$

Although the complete stoichiometry of the thermal process in eq. 21 is as yet undetermined, it does show the earmark characteristics of a radical chain process. For example attempts to determine the rate constant k_t for $Mn(CO)_3(phosphine)_2^-$ in the presence of varying amounts of Bu_3SnH led to highly irreproducible results (see Experimental). It is important to emphasize that the analogous phosphite-substituted anions $Mn(CO)_3(phosphite)_2^-$ did not afford the hydride derivatives $HMn(CO)_3(phosphite)_2$ under the same conditions, and the solutions containing Bu_3SnH remained unchanged for indefinite periods. It is also noteworthy that these two classes of carbonylmanganese anions differ primarily in their electron donor properties (see column 2, Table 1). This coupled with the radical chain character apparent in eq. 21, is indicative of electron transfer chain (ETC) catalysis [38].

Furthermore the stimulation of hydrogen transfer according to eq. 21 by a small anodic current is analogous to the electrocatalytic processes observed with other metal carbonyls [28]. The mechanistic elucidation of this interesting chain process is in progress. Despite the intrusion of the thermal process, it does not materially affect the validity of the k_2 measurement since the timescale for hydrogen transfer in eq. 21 (even with electrostimulation) is much longer than that of the DPSC experiment.

Summary and Conclusions

Electrochemistry offers convenient methods for the production of labile 17-electron carbonylmetal radicals by the anodic oxidation of readily accessible carbonylmetallates. Transient electrochemical techniques using cyclic voltammetry (CV) and double potential step chronoamperometry (DPSC) allow the ready evaluation of the reactivity of the radicals toward hydrogen transfer from tributylstannane by the measurement of the cathodic currents, as in Figs. 3 and 4, respectively. Quantitative analysis have provided the second-order rate constants k_2 for various phoshine- and phosphite-substituted carbonylmanganese radicals $Mn(CO)_3P_2^{\cdot}$ even in reactive hydrogen-donor solvents such as tetrahydrofuran. The validity of the electrochemical method is established by the comparison of the values of k_2 from DPSC analysis with those obtained earlier by Brown and McCullen using more conventional IR techniques [17].

Experimental

Materials

The carbonylmanganese complexes $Mn(CO)_5Br$, $Mn(CO)_3[(PhO)_3P]_2Br$, $Mn(CO)_3[(n\text{-}Bu)_3P]_2Br$, $Mn(CO)_3[(i\text{-}Pr)_3P]_2Br$, $Mn(CO)_3[(o\text{-}CH_3C_6H_4O)_3P]_2Br$, $Mn(CO)_3(Ph_2PCH_2)_2Br$, $Mn(CO)_3[(i\text{-}PrO)_3P]_2Br$, $Mn(CO)_3(PPh_3)_2Br$ were prepared from $Mn_2(CO)_{10}$ (Pressure Chemical Co.) as described in the literature [18,39]. The corresponding carbonylmanganate salts $NaMn(CO)_3P_2$ were prepared as air-sensitive crystals by reduction with sodium amalgam [14]. The infrared spectra of all the phosphite- and phosphine-substituted carbonylmanganate salt were highly solvent dependent [40]. The manganese hydrides $HMn(CO)_3P_2$ were prepared by the method of Ugo and Bonati [34] or by ligand substitution on $HMn(CO)_5$ [41]. The stannylmanganese carbonyls $Bu_3SnMn(CO)_3P_2$ were prepared from $NaMn(CO)_3P_2$ and tri-n-butyltin chloride (Aldrich) [15].

Tri-n-butyltin hydride was prepared by $LiAlH_4$ reduction of tri-n-butyltin chloride [42]. The deuterium-labelled Bu_3SnD was prepared similarly from 98% isotopic $LiAlD_4$ (Aldrich) and the $^2H\{^1H\}$ NMR spectrum in a THF solution containing 1 *M* $LiClO_4$ showed a singlet resonance at 4.68 (CD_3CN) with tin splittings $J(D-^{117}Sn)$ 115.2 and $J(D-^{119}Sn)$ 120.6 Hz. The IR spectrum of Bu_3SnD in THF has $\nu(Sn-D)$ 1305 cm^{-1}. Triphenylphosphine (Aldrich) was recrystallized from ethanol and dried in vacuo. 1,2-Bis-diphenylphosphinoethane (DPPE, Strem) and tri-isopropylphosphine (Aldrich, Gold Label) were used as received. Triphenyl phosphite (Aldrich), tri-isopropyl phosphite (Mobil Chemical), and tri-n-butylphosphine (M and T Chemical Co.) were refluxed over sodium and stored in Schlenk tubes after distillation in vacuo. Tetrahydrofuran (Fisher) was stirred over sodium benzophe-

none for 24 h, followed by refluxing for 5 h. It was then fractionally distilled and stored under argon in a Schlenk flask. Tetra-n-butylammonium perchlorate (TBAP, Pfaltz and Bauer) was recrystallized three times from a mixture of ethyl acetate and hexane and stored in a desiccator after drying in vacuo for 24 h.

Instrumentation

Infrared spectra were recorded on a Nicolet 10 DX FT spectrometer using 0.1 mm NaCl cells. ^{1}H NMR spectra were obtained on a JEOL FX 90Q spectrometer, and all chemical shifts are reported relative to Me_4Si. GC-MS analyses were carried out on a Hewlett-Packard 5890 chromatograph interfaced to a HP 5970 mass spectrometer (EI, 70 eV). Cyclic voltammetric measurements were performed with an IR-compensated potentiostat [43] driven by a Princeton Applied Research (PAR) 175 universal programmer. The high impedance voltage-follower amplifier was mounted external to the potentiostat for low noise pickup, and it was connected to the reference electrode with a minimum length of connection. CV curves were either displayed on a Tektronic 5115 storage oscilloscope or recorded on a Houston Series 2000 *x-y* recorder. The current axis was amplified via the potentiostat sensitivity to optimize the signal-to-noise in measuring the peak currents. The aging of the solutions was generally not a problem since we were able to reproduce the current-potential profiles throughout an experiment. The Pt working electrode was periodically polished with a very fine emery cloth. The CV cell was of air-tight design with high vacuum Teflon valves and viton O-ring seals to allow an inert atomsphere to be maintained without contamination by grease. The counter electrode which consisted of a Pt gauze was separated from the working electrode by ~ 3 mm. It was connected to the SCE reference electrode via a 0.1 μF capacitor to aid in the compensation of the *iR* drop. The double potential step chronoamperometry was carried out with the same apparatus. All inert atmosphere manipulations were carried out in a Vacuum Atmospheres dry box.

Preparative scale electrolysis

The reduction of the bromomanganese carbonyls $Mn(CO)_3P_2Br$ were carried out in an electrochemical cell of airless design equipped with a high vacuum teflon stopcock and a viton O-ring seal. This arrangement allowed the cell to accomodate a CV electrode with which to conveniently monitor the solution by cyclic voltammetry at anytime during an oxidation or reduction. The counter electrode compartment was separated from the solution by a glass frit ~ 1 mm from the working electrode. The counter electrode was constructed of a double coil of nichrome wire with a large surface area. The reference electrode compartment was separated from the solution via a salt bridge and glass frit at a distance of ~ 1 cm from the working electrode. A 0.1 μF capacitor was connected between the reference and counter electrodes to ensure higher stability. The working electrode consisted of a platinum wire cage wrapped with platinum gauze to give a total area of ~ 1.1 cm^3.

Electrochemical generation of carbonylmanganate anions $Mn(CO)_3P_2^-$

In a typical procedure, a thoroughly dried electrochemical cell was charged with an argon atmosphere. A 31 ml aliquot of a 0.3 *M* THF solution of TBAP was added to the working electrode compartment, 4 ml to the reference compartment, and 6 ml

to the counter electrode compartment and the cell was sealed. The TBAP/THF solution was then pre-reduced at the potential at which the reduction was to be carried out (~ -2.0 V vs. SCE) until there was little or no passage of current. The cell was then charged with $Mn(CO)_3[(n\text{-}Bu)_3P]_2Br$ (0.1886 g, 0.302 mmol) to give a concentration of 9.7×10^{-3} *M*. An initial CV was taken, and the solution was electrolyzed at constant potential (-2.3 V) until the passage of current ceased. In this case 58.0 C were passed which corresponded to a calculated value of 29.2 C to give $n_{app} = 1.99$. After reduction, a CV was taken. It showed the complete disappearance of the reduction wave of $Mn(CO)_3[(n\text{-}Bu)_3P]_2Br$ and only the production of $Mn(CO)_3[(n\text{-}Bu)_3P]_2NBu_4$ as evidenced by the reversible couple at -1.20 V vs. SCE. An IR spectrum after reduction also showed the complete formation of only $Mn(CO)_3[(n\text{-}Bu)_3P]_2NBu_4$. The solution afforded an identical IR spectrum as its sodium salt (vide supra) in THF. With the aid of a syringe, 4 ml of the stock solution was removed, and placed in a thoroughly dried CV cell and diluted to a total of 6 ml. The solution had a final concentration of 5×10^{-3} *M* in $Mn(CO)_3[(n\text{-}Bu)_3P]_2NBu_4$. This solution was then subjected to double step chronoamperometric analysis. The remainder of the stock solutions was diluted to 31 ml total volume and one equivalent of $HSnBu_3$ (0.079 g, 0.27 mmol) added. The solution was oxidized at a constant potential which was 150 mV more positive than that of the anodic wave of the anion/radical couple (~ -1.05 V vs. SCE) until the passage of current ceased. In this case, 8.2 C were consumed, which corresponded to the theoretical volume of 26.3 C to give $n_{app} = 0.31$. The n_{app} values for the oxidations of the anions in the presence of one equivalent of HSnBu are reported in Table 4. Immediately after electrolysis, an IR spectrum was recorded to determine the composition of the anolyte. GC-MS analysis was also undertaken at this point to determine whether $Bu_3Sn\text{-}SnBu_3$ were present. In cases where both $HMn(CO)_3P_2$- and $Bu_3Sn\text{–}Mn(CO)_3P_2$ were formed [i.e. for $P = (o\text{-}CH_3C_6H_4O)_3P$, $(PhO)_3P$, $(i\text{-}PrO)_3P$], the total areas under the most intense IR bands were calculated, and the relative amounts of the manganese hydride and tin adducts determined. The data are also reported in Table 4. The ^1H NMR spectra were used in the identification of the manganese hydrides. The workup of the solution is as follows. After oxidation of the anions $Mn(CO)_3[P]_2NBu_4$ in the presence or absence of $HSnBu_3$, the anolyte was transferred with the aid of a cannula into a 100 ml round bottom flask. The tetrahydrofuran was removed in vacuo and 20 ml of benzene was added to form a TBAP/benzene slush. Filtration through a coarse Schlenk filter funnel gave a clear homogeneous solution which was pumped to dryness. A minimum amount of C_6D_6 was added and the proton NMR spectrum recorded. Table 2 reports the chemical shifts of the manganese carbonyl hydrides obtained in this study.

Cyclic voltammetry

In a typical procedure, TBAP (1.03 g, 3.0 mmol) was dissolved in 10 ml of THF in a thoroughly dried round bottom flask under an argon atmosphere. The CV cell, after removal from a 150 °C oven and cooling in vacuo, was filled with argon and charged with $Mn(CO)_3[PPh_3]_2Br$ (0.0223 g, 0.30 mmol). A 6 ml aliquot of the THF/TBAP solution was added to the working electrode compartment and 4 ml to the reference compartment. The electrodes were inserted and cyclic voltammograms were obtained at scan rates ranging from 100 mV s^{-1} to 50 V s^{-1}. There was no evidence for electrode pollution or adsorbtion over a period of hours using the same

solution. The peak potentials and currents were calibrated by comparison with those of a ferrocene standard [44].

Deprotonation of manganese hydrides $HMn(CO)_3P_2$

The deprotonation of $HMn(CO)_3P_2$ with potassium t-butoxide was carried out as follows. In a 100 ml round bottom flask equipped with a stopcock was added 15 ml of thoroughly dried and degassed acetonitrile and potassium t-butoxide (Alfa Chemical) (0.5 g, 4.46 mmol) under an argon atmosphere to form a heterogeneous solution. $HMn(CO)_3[PPh_3]_2$ (0.30 g, 0.45 mmol) was added, and the solution stirred vigorously. Over a period of 3 h, the color of the solution changed from colorless to the orange of $Mn(CO)_3[PPh_3]_2^-$. Filtration through a medium Schlenk filter funnel afforded a homogeneous solution, and the addition of 100 ml of Et_2O afforded an orange solid. Isolation of the $KMn(CO)_3[PPh_3]_2$ and dissolution in THF afforded an IR spectrum which was the same as that of the sodium and tetra-n-butylammonium salts described above.

Double potential step chronoamperometry

Typically, a 6 ml aliquot of a 5×10^{-3} M solution of the carbonylmanganate $Mn(CO)_3P_2^-$ was added to the CV cell under an inert atmosphere. The PAR programmer was set up to provide an anodic potential pulse which was 100 mV more positive than that of the anodic wave of the $Mn(CO)_3P_2^-/Mn(CO)_3P_2^{\cdot}$ couple. The duration of the pulse θ was typically varied from $\theta = 0.3$, 0.5, 1, 2, 3, 5 to 10 s. After θ s, the potential was stepped to a new value which was 100 mV more negative of the cathodic peak of the above couple. It was held at this potential for the same time θ, and the current ratio $[i_c(2\theta)/i_a(\theta)]$ calculated. The identical procedure was followed in the presence of varying amounts of added $HSnBu_3$, and the current ratios again measured. The concentration of $HSnBu_3$ was varied incrementally from 0.5 to 20 equivalents with respect to anion concentration and the amount depended on the rate of hydrogen atom abstraction. The plot of $[i_c(2\theta)/i_a(\theta)]/0.293$ vs. $\log([HSnBu_3]\theta)$ gave smooth curves similar to those shown in Fig. 5. The direct comparison of the experimental and theoretical curves gave the rate constant for hydrogen atom abstraction k_2 in M^{-1} s^{-1}.

In order to develop the theoretical working curve for the DPSC experiment, we considered the most general mechanism to be one which involves Scheme 2 and includes the stannyl dimerization, i.e.

$$2Bu_3Sn^{\cdot} \xrightarrow{k_4} Bu_3SnSnBu_3 \qquad (22)$$

Dimensional analysis [45] shows that the kinetic behavior based on this scheme depends on three parameters, viz., $\lambda = k_2[Bu_3SnH]\theta$, $\sigma = k_{-2}/k_3$ and $\gamma = k_2k_4/k_3^2[Bu_3SnH]/C^0$, where θ is the duration of the pulse width and C^0 the initial concentration of the carbonylmanganate. Experimentally we found that the DPSC data were independent of C^0 within the experimental error. This result shows that δ should not play a decisive role on the overall kinetic behavior. By kinetic analysis this is true only if either eq. 17 is irreversible or eq. 22 is not involved. The numerical resolution of the pertinent set of partial differential equations and boundary conditions [46] allows the theoretical working curves which correspond to each of these kinetic situations to be drawn. Curve fitting the experimental data

shows that the mechanism with eq. 17 irreversible gives no agreement, and it must be rejected accordingly. However, the theoretical working curve based on the mechanism in Scheme 2 involving the partial equilibration of eq. 17 gives good agreement with the experimental data, as shown in Fig. 5. The determination of k_2 and $\sigma = k_{-2}/2k_3$ was possible for all $Mn(CO)_3P_2^{\cdot}$ listed in Table 5, except those where P = PPh_3 and $(i\text{-}Pr)_3P$. With these bulky phosphines the use of large amounts of Bu_3SnH were necessary to observe the requisite decrease in the cathodic current. This resulted in large background currents and excessive scatter. If these data were forced to fit the working curves, almost coincident fits were obtained for P = PPh_3 and $i\text{-}Pr_3P$ provided $\log\sigma$ was greater than 1.0 and 1.5, respectively. This leads to the maximum values of $k_2 = 0.6$ and 0.01 M^{-1} s^{-1} for $Mn(CO)_3(PPh_3)_2^{\cdot}$ and $Mn(CO)_3(i\text{-}Pr_3P)_2^{\cdot}$ respectively. Owing to the large values of σ (which indicates that eq. 17 actually acts as a rapid preequilibrium), a new working curve was derived for the limiting situation $\sigma \rightarrow \infty$. Though some scatter was observed, reasonable fits to the new working curve with the parameter $\sigma' = k_2/k_3/k_{-2}$ were obtained. The values of $\sigma' = 4.6 \times 10^{-2}$ and 6×10^{-2} M^{-1} s^{-1} for $Mn(CO)_3(PPh_3)_2^{\cdot}$ and $Mn(CO)_3(i\text{-}Pr_3P)_2$ reflect the large size of these phosphorus ligands to be a major factor which affects the decreased homolytic reactivity of these radicals.

Kinetic isotope effect in the reactivity of $Mn(CO)_3P_2$

The deuterium isotope effect in hydrogen atom transfer to $Mn(CO)_3P_2^{\cdot}$ was examined with those derivatives in which P = $(i\text{-}PrO)_3P$ and DPPE. The DPSC experiments were carried out with the isotopically labelled tributylstannane [47] in the manner described above. For $Mn(CO)_3[(i\text{-}PrO)_3P]_2^-$ the DPSC experiments were carried out in the presence of 2, 4, 8 and 12 equivalents of Bu_3SnD to yield $k_2 = 4.6$ M^{-1} s^{-1} and $\log\sigma = -0.5$. Product analysis from the bulk electrolysis of $Mn(CO)_3[(i\text{-}PrO)_3P]_2^-$ in the presence of 1 equiv. of Bu_3SnD indicated the complete conversion to $DMn(CO)_3[(i\text{-}PrO)_3P]_2$ (50%) and $Bu_3SnMn(CO)_3[(i\text{-}PrO)_3P]_2$ (50%) with the consumption of 1-electron per mole of carbonylmanganate. The ν(CO) bands in the IR spectrum of $DMn(CO)_3[(i\text{-}PrO)_3P]_2$ were the same as those of the protio analog (Table 2). The $^2H\{^1H\}$ NMR spectrum showed a broad 1/2/1 triplet contained at -8.6 ppm (CD_3CN) with J(P–D) 4 Hz in THF containing 1 M $LiClO_4$. No resonance at this chemical shift was observed in the ^1H NMR spectrum.

The DPSC experiment with $Mn(CO)_3(DPPE)_2^-$ was carried out with 0.5, 1.5 and 3 equiv. of Bu_3SnD to yield $k_2 = 28$ M^{-1} s^{-1} and $\log\sigma = -1.0$. Bulk oxidation of $Mn(CO)_3(DPPE)^-$ in the presence of 1 equiv. of Bu_3SnD consumed 0.5 electrons per mole of carbonylmanganate and produced $DMn(CO)_3(DPPE)$ (100%) by IR analysis of the anolyte. The $^2H\{^1H\}$ NMR spectrum showed a broad 1/2/1 triplet resonance centered at -8.15 ppm (CD_3CN) with J(P–D) 7.8 Hz. A small signal of $HMn(CO)_3(DPPE)$ was also observed in the ^1H NMR spectrum. The ratio of the deutero/protio manganese carbonyls was estimated to be 7/3.

Hydrogen transfer to carbonylmanganate anions

The carbonylmanganate anions (5×10^{-3} M) with P = n-Bu_3P, PPh_3 and DPPE were treated with one equiv. Bu_3SnH in THF containing 0.3 M TBAP. Analysis of the mixture after 12 h for P = DPPE, 24 h for P = n-Bu_3P and 72 h for P = PPh_3 indicated quantitative yields of the manganese hydrides $HMn(CO)_3P_2$ by IR analyses. Large but unquantified yields of $Bu_3SnSnBu_3$ were also observed by

GC-MS analysis. Small amounts of another tin-containing product X was observed with $P = PPh_3$.

When the corresponding carbonylmanganates were treated with Bu_3SnCl, an immediate reaction ensued even at $-78°C$. IR analysis indicated the manganese hydride to be formed in quantitative yields together with major amounts of the tin-containing product X (vide supra) and small amounts of $Bu_3SnSnBu_3$. GC-MS analysis of X gave one major tin-containing peak at $m/z = 313$. An important isotopic tin envelope was readily apparent and separated by 57 mass units (-Bu) at $m/z = 199$. In addition two minor tin envelopes at $m/z = 177$ and 119 were apparent. When a freshly distilled pure sample of Bu_3SnCl was subjected to the same GC/MS analysis an intense peak at $m/z = 267$ was observed for Bu_2SnCl^+ together with the mass spectrum of X described above.

A preliminary kinetic investigation was carried out with $Mn(CO)_3(Bu_3P)_2^-$ and various amounts of Bu_3SnH. The disappearance of the carbonylmanganate followed by cyclic voltammetry obeyed first-order kinetics. However, the observed first-order rate constant varied irreproducibly by at least an order of magnitude. No direct relationship between the rate constant and the tin hydride or carbonylmanganate concentration was discerned.

CV simulation of carbonylmanganate oxidation in the presence of Bu_3SnH

The matrix of cyclic voltammograms in Fig. 3 was simulated by the finite difference method of Feldberg [48]. The computer simulations were based on the simple EC mechanism included in Scheme 1 by using only eqs. 10 and 11. The appropriate boundary conditions and differential equations for the CV simulation was given previously [45].

Acknowledgment

We thank the National Science Foundation and the Robert A. Welch Foundation for financial support. This research was also carried out under the auspices of the U.S.-France Cooperative Research Program jointly sponsored by NSF and CNRS.

References

1 T.L. Brown, Ann. N.Y. Acad. Sci., 80 (1980) 333.
2 J.K. Kochi, J. Organomet. Chem., 300 (1986) 139.
3 (a) J.W. Hershberger, R.J. Klingler, and J.K. Kochi, J. Am. Chem. Soc., 104 (1982) 3034; 105 (1983) 61; (b) B.A. Narayanan, C. Amatore, and J.K. Kochi, J. Chem. Soc., Chem. Commun., (1983) 397; (c) J.W. Hershberger, C. Amatore, and J.K. Kochi, J. Organomet. Chem., 250 (1983) 345.
4 D.J. Kuchynka, C. Amatore and J.K. Kochi, Inorg. Chem., 25 (1986) 4087.
5 (a) R.E. Dessy and P.M. Weissman, J. Am. Chem. Soc., 88 (1966) 5124; (b) R.E. Dessy, R.B. King, and M. Waldrop, J. Am. Chem. Soc., 88 (1966) 5112; (c) R.E. Dessy and R.L. Pohl, J. Am. Chem. Soc., 90 (1968) 2005.
6 J.A. Armstead, D.J. Cox and R. Davis, J. Organomet. Chem., 236 (1982) 213.
7 (a) R.B. King, Adv. Organomet. Chem., 2 (1964) 157; (b) J.E. Ellis, J. Organomet. Chem., 86 (1975) 1; (c) J.E. Ellis and E.A. Flom, J. Organomet. Chem., 99 (1975) 263; (d) R.B. King, Acc. Chem. Res., 3 (1970) 417.
8 (a) J.A. Gladysz, G.M. Williams, W. Tam, and D.L. Johnson, J. Organomet. Chem., 140 (1977) C1; (b) K. Inkrott, R. Goetze and S.G. Shore, J. Organomet. Chem., 154 (1978) 337; (c) D.H. Gibson, F.U. Ahmed and K.R. Phillips, J. Organomet. Chem., 206 (1981) C17.

9 (a) R.E. Dessy, F.E. Stary, R.B. King and M. Waldrop, J. Am. Chem. Soc., 88 (1966) 471; (b) R.E. Dessy, R.B. King and M. Waldrop, J. Am. Chem. Soc., 88 (1966) 5112; (c) R.E. Dessy, P.M. Weissman and R.L. Pohl, J. Am. Chem. Soc., 88 (1966) 5117.

10 (a) N. El Murr and A. Chaloyard, Inorg. Chem., 21 (1982) 2206; (b) P. Lemoine, A. Giraudeau and M. Gross, Electrochim. Acta, 21 (1976) 1.

11 (a) C.J. Pickett and D. Pletcher, J. Chem. Soc., Dalton Trans., (1975) 879; (b) C.J. Pickett and D. Pletcher, J. Chem. Soc., Dalton Trans., (1976) 749.

12 E.O. Brimm, M.A. Lynch and W.J. Sesny, J. Am. Chem. Soc., 76 (1954) 3831.

13 R.B. King and F.G.A. Stone, Inorg. Synth., 7 (1963) 196.

14 (a) W. Hieber, M. Hofler and J. Muschi, Chem. Ber., 98 (1965) 311; (b) W. Hieber, G. Faulhaber and F.Z. Theubert, Z. Anorg. Allg. Chem., 314 (1962) 125; (c) W. Hieber, G. Faulhaber and F.Z. Theubert, Z. Naturforsch B, 15 (1960) 326.

15 (a) S. Onaka, Y. Yoshikawa and H. Yamatera, J. Organomet. Chem., 157 (1978) 187; (b) W. Jetz, P.B. Simons, J.A. Thompson and W.A.S. Graham, Inorg. Chem., 5 (1966) 2217; (c) R.A. Burnham and S.R. Stobert, J. Chem. Soc., Dalton Trans., (1973) 1269.

16 (a) R.A. Faltynek and M.S. Wrighton, J. Am. Chem. Soc., 100 (1978) 2701; (b) P.M. Treichel and J.J. Benedict, J. Organomet. Chem., 17 (1969) P37.

17 T.L. Brown and S.B. McCullen, J. Am. Chem. Soc., 104 (1982) 7496.

18 R.J. Angelici, F. Basolo and A.J. Poë, J. Am. Chem. Soc., 85 (1963) 2215.

19 (a) J.H. Christie, J. Electroanal. Chem., 13 (1967) 79; (b) R.S. Nicholson and J.T. Lundquist, J. Electroanal. Chem., 16 (1968) 445.

20 (a) S.W. Feldberg and L. Jeftic, J. Phys. Chem., 76 (1972) 2439; (b) I. Shain and W.M. Schwarz, J. Phys. Chem., 69 (1965) 30.

21 (a) C.A. Amatore, D. Garreau, M. Hammi, J. Pinson and J.M. Saveant, J. Electroanal. Chem., 184 (1985) 1; (b) C.P. Andrieux, P. Hapiot and J. M. Saveant, J. Electroanal. Chem., 172 (1984) 49.

22 (a) A. Lasia, J. Electroanal. Chem., 146 (1983) 397; (b) K.B. Oldham, J. Electroanal. Chem., 145 (1983) 9; (c) D.H. Evans and M.J. Kelly, Anal. Chem., 54 (1982) 1727.

23 A.J. Bard and L.A. Faulkner, Electrochemical Methods, Wiley, New York, 1980, p. 181.

24 L. Nadjo and J.M. Saveant, J. Electroanal. Chem., 48 (1973) 113.

25 (a) S.B. McCullen, H.W. Walker and T.L. Brown, J. Am. Chem. Soc., 104 (1982) 4007; (b) D.R. Kidd, C.P. Cheng and T.L. Brown, J. Am. Chem. Soc., 100 (1978) 4103.

26 B.A. Narayanan, C. Amatore and J.K. Kochi, Organometallics, in press.

27 R.J. Klingler, J.C. Huffman and J.K. Kochi, Inorg. Chem., 20 (1981) 34.

28 (a) F. M'Halla, J. Pinson and J.M. Saveant, J. Am. Chem. Soc. 102, (1980) 4120. (b) See also, B.A. Narayanan, C. Amatore and J.K. Kochi, Organometallics, 5 (1986) 926.

29 Compare J. Lusztyk, E. Lusztyk, B. Maillard, L. Lunazzi and K.U. Ingold, J. Am. Chem. Soc., 105 (1983) 4475.

30 D.J. Carlsson and K.U. Ingold, J. Am. Chem. Soc., 90 (1968) 7047.

31 Compare ref. 3.

32 R.S. Nicholson and I. Shain, Anal. Chem., 36 (1964) 706.

33 R.L. Harlow, P.J. Krusic, R.L. McKinney and S.S. Wreford, Organometallics, 1 (1982) 1506.

34 R. Ugo and F. Bonati, J. Organomet. Chem., 8 (1967) 189.

35 (a) M.L. Olmstead and R.S. Nicholson, Anal. Chem., 41 (1969) 851; (b) M.K. Hanafey, R.L. Scott, T.H. Ridgway and C.N. Reilley, Anal. Chem., 50 (1978) 116; (c) V.D. Parker, Acta Chem. Scand. Ser. B, B37 (1983) 871; (d) ibid., B37 (1983) 597; (e) A.J. Bellamy, J. Electroanal. Chem., 158 (1983) 69; (f) T. Ohsaka, T. Sotomura, H. Matsuda and N. Oyama, Bull. Chem. Soc. Japan, 56 (1983) 3065; (g) C.A. Amatore and J.M. Saveant, J. Electroanal. Chem., 102 (1979) 21; (h) R. Seeber and S. Stefani, Anal. Chem., 53 (1981) 1011; (i) W.V. Childs, J.T. Maloy, C.P. Keszthelyi and A.J. Bard, J. Am. Chem. Soc. Div. Petrol. Chem. Preps., 15 (1970) B38; (j) T.H. Ridgway, R.P. Van Duyne and C.N Reilly, J. Electroanal. Chem., 69 (1976) 165.

36 C.A. Tolman, Chem. Rev., 77 (1977) 313.

37 R.A. Jackson and A. Poë, Inorg. Chem., 17 (1978) 997. See also J.L. Goodman, K.S. Peters and V. Vaida, Organometallics, 5 (1986) 815.

38 See H.H. Ohst and J.K. Kochi, J. Am. Chem. Soc., 108 (1986) 2897 and references therein.

39 E.W. Abel and G. Wilkinson, J. Chem. Soc., (1959) 1501.

40 (a) D.J. Darensbourg and M.Y. Darensbourg, Inorg. Chim. Acta, 5 (1971) 247; (b) M.Y. Darensbourg and J.M. Hanckel, J. Organomet. Chem., 217 (1981) C9; (c) S.C. Kao, M.Y. Darensbourg and W. Schenk, Organometallics, 3 (1984) 871 and references therein.

41 R.J. Ruszczyk, H. Bih-Lian and J.D. Atwood, J. Organomet. Chem., 299 (1986) 205.
42 G.J.M. van der Kerk, J.G. Noltes and J.G.A. Luijten, J. Appl. Chem., 7 (1957) 366.
43 D. Garreau and J.M. Saveant, J. Electroanal. Chem., 35 (1972) 309; ibid., 50 (1974) 1.
44 R.R. Gagne, C.A. Koval and G.C. Lisensky Inorg. Chem., 19 (1980) 2854.
45 See P.M. Zizelman, C. Amatore and J.K. Kochi, J. Am. Chem. Soc., 106 (1984) 3771.
46 Manuscript in preparation.
47 W.P. Neumann and R. Sommer, Angew. Chem., 75 (1963) 788. W.P. Neumann and H.J. Sommer, Synthesis, (1980) 942.
48 S.W. Feldberg in A.J. Bard (Ed.), Electroanalytical Chemistry, Dekker, New York, 1969, p. 199 ff. S.W. Feldberg in H.B. Mark (Ed.), Computer Application in Analytical Chemistry, Dekker, New York, 1972, Vol. 2, Ch. 7.